Oncogene (2017) **36**, 3274–3286

www.nature.com/onc

OPEN

ORIGINAL ARTICLE

Unbalancing p53/Mdm2/IGF-1R axis by Mdm2 activation restrains the IGF-1-dependent invasive phenotype of skin melanoma

C Worrall[1], N Suleymanova[1], C Crudden[1], I Trocoli Drakensjö[1,2], E Candrea[1,3], D Nedelcu[1], S-I Takahashi[4], L Girnita[1] and A Girnita[1,2]

Melanoma tumors usually retain wild-type p53; however, its tumor-suppressor activity is functionally disabled, most commonly through an inactivating interaction with mouse double-minute 2 homolog (Mdm2), indicating p53 release from this complex as a potential therapeutic approach. P53 and the tumor-promoter insulin-like growth factor type 1 receptor (IGF-1R) compete as substrates for the E3 ubiquitin ligase Mdm2, making their relative abundance intricately linked. Hence we investigated the effects of pharmacological Mdm2 release from the Mdm2/p53 complex on the expression and function of the IGF-1R. Nutlin-3 treatment increased IGF-1R/Mdm2 association with enhanced IGF-1R ubiquitination and a dual functional outcome: receptor downregulation and selective downstream signaling activation confined to the mitogen-activated protein kinase/extracellular signal-regulated kinase pathway. This Nutlin-3 functional selectivity translated into IGF-1-mediated bioactivities with biphasic effects on the proliferative and metastatic phenotype: an early increase and late decrease in the number of proliferative and migratory cells, while the invasiveness was completely inhibited following Nutlin-3 treatment through an impaired IGF-1-mediated matrix metalloproteinases type 2 activation mechanism. Taken together, these experiments reveal the biased agonistic properties of Nutlin-3 for the mitogen-activated protein kinase pathway, mediated by Mdm2 through IGF-1R ubiquitination and provide fundamental insights into destabilizing p53/Mdm2/IGF-1R circuitry that could be developed for therapeutic gain.

Oncogene (2017) **36,** 3274–3286; doi:10.1038/onc.2016.472; published online 16 January 2017

INTRODUCTION

Melanoma is the most deadly form of skin cancer, and strikingly, its incidence has doubled over the past four decades in Western populations. Although treatable by surgery at early stages, the disease has a high propensity to metastasize and clinical outcome from this stage results in a 5-year survival rate $< 20\%$.[1]

Melanoma originates from melanocytes in the skin, specialized pigment-producing cells that buffer and shield the body against the damaging effects of ultraviolet (UV) radiation. Hence, melanoma development is intricately connected to UV exposure.[2] It is perhaps not surprising that large-scale sequencing studies have established melanoma as among the cancers with the highest mutation load, thus correlating its pathogenicity with the molecular signatures of UV damage.[3] Yet, what makes melanoma stand out within this group of high mutation load cancers is the low mutation frequency of the p53 gene.[4] In contrast to other cancer types with similar mutation loads such as lung and colon cancers, in which p53 is mutated in about 80–90% of cases, only 10–20% of malignant melanomas contain somatic mutations in the TP53 gene.[5–7]

The tumor-suppressor p53 prevents carcinogenesis by maintaining genetic stability through activating DNA repair mechanisms, inducing growth arrest and, if damage severity is beyond repair, initiating apoptosis.[8] In an unstressed environment, p53 is kept at low levels by its natural inhibitor Mdm2 (mouse double-minute 2 homolog) through at least two main mechanisms: the direct binding of Mdm2 to the N-terminal end of p53 hinders its nuclear translocation and transcriptional activation, while the Mdm2 E3 ubiquitin ligase targets p53 for degradation through the 26S proteasome.[9] When confronted with cellular stress of various types, including UV radiation and oncogene activation, the Mdm2/p53 interaction is prevented leading to an extended half-life and enhanced p53 transcriptional activity. The system is returned to its low p53 equilibrium through a negative feedback loop, as p53 transcriptionally increases Mdm2.[10]

Mdm2 was originally identified as being gene-amplified on double-minute chromosomes in transformed mouse fibroblasts,[11] and in line with its well-characterized role as a negative regulator of the tumor-suppressor p53, it is traditionally defined as an oncogene. Nevertheless, there is growing evidence suggesting the possibility that in the appropriate context Mdm2 can also exert inhibitory effects on cell proliferation thus acting as a tumor suppressor (for an extensive review, see Manfredi[12]). Although the molecular basis underlying the growth-suppressing function of Mdm2 is far from being elucidated, one possible area of research, as related to its ubiquitin-ligase function, is that, in addition to p53, Mdm2 directly ubiquitinates and degrades other substrates. Within this theme, we described the involvement of Mdm2 in ubiquitination of the tumor-promoting insulin-like growth factor type 1 receptor (IGF-1R).[13] We proved that Mdm2

[1]Department of Oncology and Pathology, Cancer Center Karolinska, Karolinska Institute, Karolinska University Hospital, Stockholm, Sweden; [2]Dermatology Department, Karolinska University Hospital, Stockholm, Sweden; [3]Department of Dermatology, University of Medicine and Pharmacy 'Iuliu Hatieganu' Cluj-Napoca, Romania and [4]Departments of Animal Sciences and Applied Biological Chemistry, Graduate School of Agriculture and Life Sciences, The University of Tokyo, Tokyo, Japan. Correspondence: Professor L Girnita or Dr A Girnita, Department of Oncology-Pathology, Cancer Center Karolinska, Karolinska Institute, Karolinska University Hospital, CCK R8:04, Stockholm S-17176, Sweden.

E-mail: Leonard.Girnita@ki.se or Ada.Girnita@ki.se

Received 29 July 2016; revised 24 October 2016; accepted 31 October 2016; published online 16 January 2017

physically associated with and directly caused ubiquitination with subsequent degradation as well as downstream signaling activation of the IGF-1R and this effect was independent of the p53 status (that is, wild type or mutated).[14–16] As for many other tumor types, IGF-1R has been demonstrated to have a central role in the progression and maintenance of the malignant phenotype of melanoma cells. This includes autocrine stimulation through IGF-1 ligand/IGF-1R,[17] apoptosis prevention through activation of phosphatidylinositol 3′-kinase (PI3K) and mitogen-activated protein kinase (MAPK) pathways,[18] even in tumors expressing activating downstream RAS/RAF mutations.[19] In particular, IGF-1R has been shown to have a crucial role in melanoma cell invasion and metastasis[20,21] and anti-IGF-1R therapy has shown partial response in advanced melanoma patients.[22–26]

Most malignant melanoma tumors retain wild-type p53 (wtp53)[5–7] and have instead developed alternative mechanisms, most commonly overproduction of Mdm2, for disabling p53 expression and function.[27–29] Small-molecule inhibitors have been developed with the aim of reactivating p53 by preventing its interaction with Mdm2. Nutlin-3 is one such small-molecule inhibitor, a *cis*-imidazoline analog, which binds to Mdm2 in the p53-binding pocket, thus preventing Mdm2-mediated p53 degradation, stabilizing p53 and additionally increasing its synthesis rate causing growth arrest.[30–34] Nutlin-3 has been studied in various cancer models, including melanoma,[35] yet all studies thus far have investigated exclusively the effects of p53 reactivation on cancer cell proliferation and survival. The aim of the present study is to specifically investigate the effects of Mdm2 reactivation following pharmacological disruption of the Mdm2/p53 complexes, focusing on another cancer relevant Mdm2 substrate, the IGF-1R, in the context of the malignant phenotype of melanoma cells.

RESULTS

Effects of Nutlin-3 on mutant and wtp53 melanoma cells

Nutlin-3 is known to increase p53 levels by blocking its binding to Mdm2. In turn, as long as the downstream p53 pathway is not otherwise disabled, Mdm2 accumulates through p53 transcriptional activation. Aiming to investigate the effects of Mdm2 accumulation, the first experiments were designed to identify the dose high enough to induce Mdm2, yet with minimal p53-mediated effects on cell viability. We used a panel of melanoma cell lines with known p53 status: two wtp53 cell lines, DFB and MelJuSo, and two mutant (mtp53) cell lines, BE and SK-Mel28 (termed Mel28 throughout).

Initial characterization of the cell panel by western blotting (WB) analysis showed high basal p53 levels in the mtp53 BE and Mel28 cells relative to lower levels of p53 protein in the wtp53 cells DFB and MelJuSo (Figure 1a). Mdm2 is correspondingly low in the mtp53 cells and relatively high in the wtp53 cells (Figure 1a). In line with their p53 status, 3 days of treatment with micromolar concentrations of Nutlin-3 decreases the cell viability of wtp53 melanoma cells in a time- and dose-dependent manner while mtp53 cells were not (Mel28) or only slightly affected by high doses (BE; Figure 1b). Submicromolar Nutlin-3 treatment showed no significant effect on cell viability in any of the cell lines (data not shown). Based on these experiments, a Nutlin-3 concentration of 1 μM, demonstrating minimal p53 proapoptotic effects within 48 h, was chosen for subsequent experiments.

Nutlin-3 treatment stabilizes Mdm2 and downregulates IGF-1R

IGF-1R is a major ubiquitination substrate competing with p53 for the ubiquitin ligase Mdm2.[13,36–41] Following ligand stimulation, the adaptor protein β-arrestin 1 or -2 is recruited to the receptor C-terminal, mediating Mdm2 binding, receptor ubiquitination and degradation.[15,42,43]

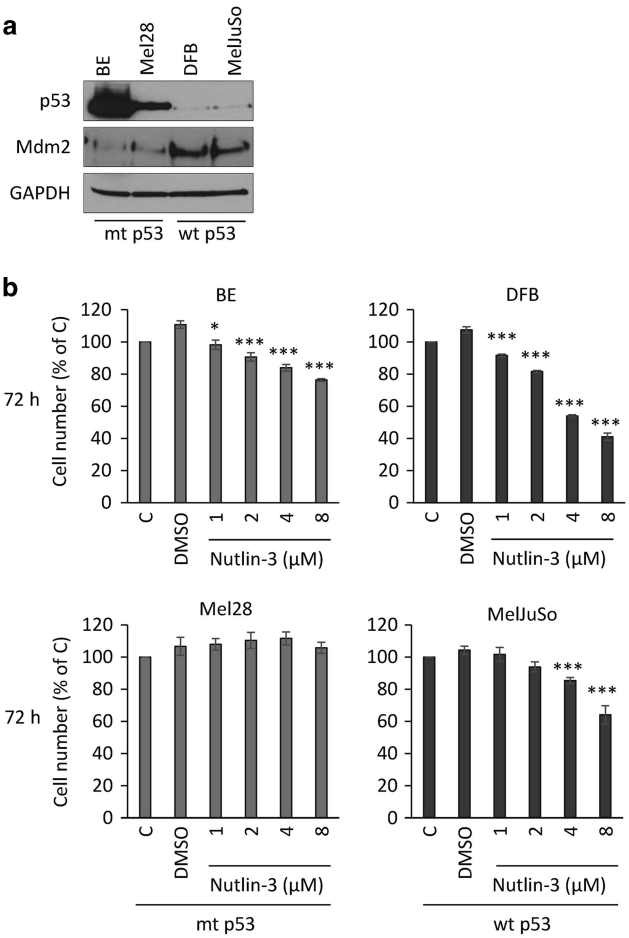

Figure 1. Effects of Nutlin-3 on mutant and wtp53 melanoma cells. (**a**) Cell lysates were prepared from melanoma cell lines grown in complete media and analyzed by WB for p53, Mdm2 and GAPDH as a loading control. The cell line p53 status is indicated as mtp53 or wtp53. (**b**) Cell viability of the Nutlin-3-treated cells as indicated, was evaluated by PrestoBlue assay and displayed as a percentage of untreated controls. Data correspond to the mean ± s.e.m. from three independent experiments. Statistical analysis: Nutlin-3-treated cells compared with control-treated cells: $^{*}P < 0.05$, $^{***}P < 0.001$.

Nutlin-3 binds at the p53-binding pocket at the N-terminal of Mdm2 (amino acids (aa) 26–108),[32] whereas β-arrestin 1/IGF-1R binds to Mdm2 between aa 161 and 400,[42–44] therefore Nutlin-3 should not prevent β-arrestin 1/Mdm2 interaction (Figure 2a). Thus, in the next experiments, we evaluated the effects of Nutlin-3 on IGF-1R expression. As demonstrated in Figure 2b, in wtp53 DFB cells, p53 and Mdm2 accumulate in a dose-dependent manner with a simultaneous decrease in IGF-1R expression. In the mtp53 cell line BE, the level of observed Mdm2 accumulation is lower than in the wtp53 cell lines and no significant changes in p53 nor IGF-1R were observed after 24 h of treatment. Similarly, a single dose (1 μM) with different durations of treatment causes wtp53 cells to decrease IGF-1R expression alongside Mdm2 accumulation, while in mtp53 BE cells, IGF-1R downregulation is slower and occurs to a much lesser extent (Figure 2c), with a parallel increase in Mdm2 levels. The wtp53 cell line MelJuSo demonstrated Nutlin-3-induced IGF-1R downregulation, while the second mtp53 cell line Mel28 showed no changes in Mdm2, p53 or IGF-1R following Nutlin-3 treatment (Figure 2d). Together this data suggest that Nutlin-3 causes decreases in IGF-1R in wtp53 cells alongside the Mdm2 accumulation, while in mtp53 cells these effects are

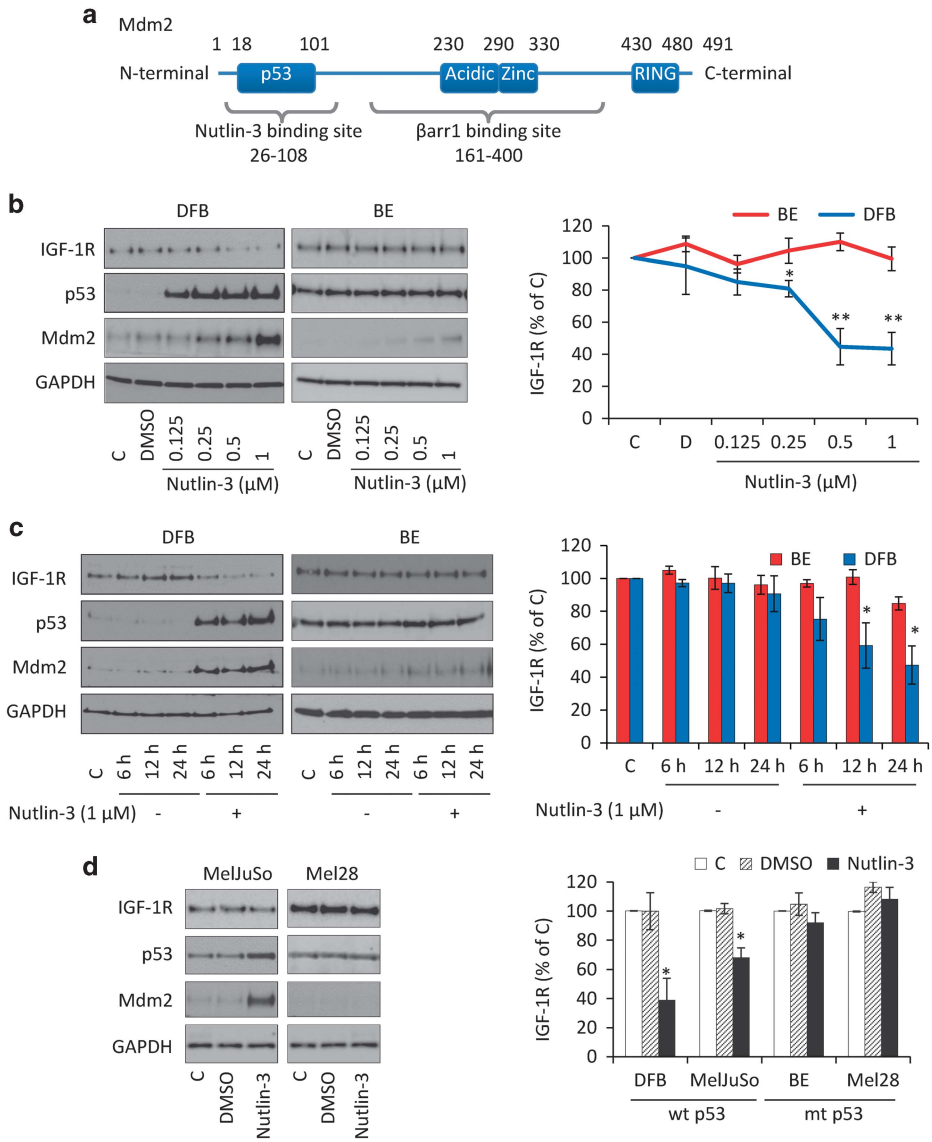

Figure 2. Nutlin-3 treatment stabilizes Mdm2 and downregulates IGF-1R. (**a**) Mdm2 functional and binding domains. Diagram indicating the known functional domains and the limits of regions interacting with Nutlin-3 and β-arr1/IGF-1R. (**b**–**d**) Dose (**b**) and time (**c**) dependent effects of Nutlin-3 treatment on p53, Mdm2 and IGF-1R expression. Cells incubated in serum were treated with Nutlin-3 as indicated. Protein lysates were analyzed by WB for IGF-1R, p53, Mdm2 and GAPDH as a loading control (left panels). IGF-1R signals were quantified by densitometry, normalized to GAPDH and expressed as a percentage of the IGF-1R in the control-treated cells (right panels). Data correspond to the mean ± s.e.m. from three independent experiments. Statistical analysis: Nutlin-3-treated cells compared with control-treated cells: $*P < 0.05$, $**P < 0.01$.

delayed or absent, possibly owing to not reaching a critical level of Mdm2 (Figure 2d).

Ligand dependency of Nutlin-3 effects on IGF-1R downregulation

Under physiological conditions, as with many other receptor tyrosine kinases, only ligand-occupied IGF-1R is degraded,[41,45] although non-canonical degradation with non-classical ligands is recognized.[39,40,44,46] Hence, we next tested whether ligand–receptor interaction was essential for Nutlin-3-mediated IGF-1R degradation. Serum-starved cells were treated with Nutlin-3 for 6 h, stimulated or not with IGF-1, and analyzed for p53, Mdm2 and IGF-1R level by WB (Figure 3a). In the wtp53 cell lines, Nutlin-3 treatment results in the accumulation of both p53 and Mdm2, with the latter being increased more in the presence of IGF-1. Intriguingly and confirming the results in Figure 2b, Nutlin-3 treatment also causes accumulation of Mdm2 in a dose-dependent manner in both mtp53 cell lines, without modifying p53 levels (Figure 3a, right panels), again more noticeable with IGF-1 stimulation.

The ligand and Nutlin-3 dose dependency was confirmed by densitometric quantification of the WB analysis across multiple experiments (Figure 3b). The mtp53 cell line BE showed a trend toward Nutlin-3-dependent IGF-1R degradation in the presence of IGF-1 but only displayed a 20% decrease at 1 μM Nutlin-3 concentration, which did not reach statistical significance.

Mechanism of Nutlin-3-dependent IGF-1R downregulation

The promoter region of the IGF-1R gene contains multiple potential binding sites for known onco-proteins and tumor suppressors,[47] and it has long been recognized that wtp53 interacts with the IGF-1R promoter and negatively regulates its transcription.[48–50] Hence, our next aim was to investigate whether the Nutlin-3-mediated reduction in IGF-1R was due to p53-mediated IGF-1R transcriptional inhibition

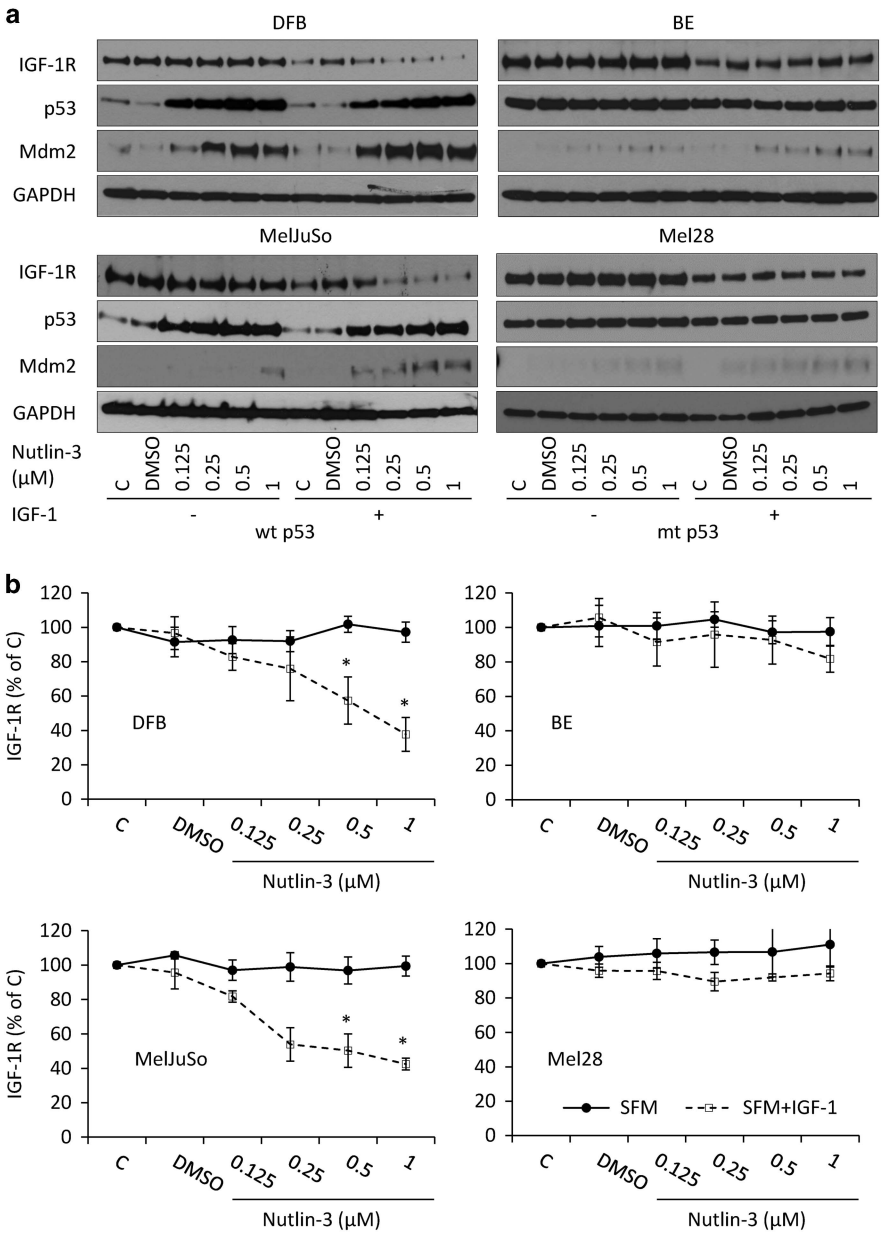

Figure 3. Ligand dependency of Nutlin-3 effects on IGF-1R downregulation. (**a**) Cells were plated, allowed to attach and treated as indicated in serum-free media for 6 h and then stimulated or not with IGF-1 (50 ng/ml) for 12 h. Total cell lysates were analyzed by WB for IGF-1R, Mdm2, p53 and GAPDH as a loading control. (**b**) IGF-1R levels were quantified by densitometry, normalized to GAPDH and expressed as a percentage of the IGF-1R levels in the control-treated cells. Data correspond to the mean ± s.e.m. from three independent experiments. Statistical analysis (two-tailed *T*-test): Nutlin-3-treated cells compared with control-treated cells: $^*P < 0.05$.

or Mdm-2-mediated IGF-1R ubiquitination and degradation at the posttranslational level.

Real-time quantitative reverse transcription-PCR (qRT-PCR) confirmed that 1 μM of Nutlin-3 treatment for 24 h caused no changes in IGF-1R mRNA level in any of the tested cell lines (Figure 4a). In addition, WB analysis of the pro-IGF-1R (new protein en route to the cell surface) further confirmed that levels of newly synthesized IGF-1R were unchanged by Nutlin-3 (data not shown). Together, this suggests that Nutlin-3 IGF-1R downregulation is mediated through an increased degradation mechanism rather than decreased synthesis. To fully validate this mechanism, we investigated whether the IGF-1R physically associates with and is ubiquitinated by Mdm2 following Nutlin-3 treatment.

Direct protein association was tested by immunoprecipitation (IP) of IGF-1R and WB detection for the putative associated protein. This was performed without and with Nutlin-3 treatment for 6 h in the presence or absence of 10 min IGF-1 stimulation (Figure 4b), allowing us to test whether we could detect basal association of the proteins and whether the interaction altered with ligand-mediated receptor conformational changes. In serum-starved conditions, recruitment of Mdm2 to the IGF-1R could be detected but at very low levels and greatly increased after IGF-1, indicating a ligand-dependent mechanism (Figure 4b). Nutlin-3 treatment enhanced Mdm2 recruitment to IGF-1R, even in the absence of the ligand, suggesting that Mdm2 released from p53 by Nutlin-3 is available for binding to the IGF-1R. Ligand stimulation further increases Nutlin-3-induced IGF-1R/Mdm2. WB analysis of whole-cell lysates prior to IP confirmed equal IGF-1R among the treatment conditions and indicates the relative Mdm2 levels (Figure 4b).

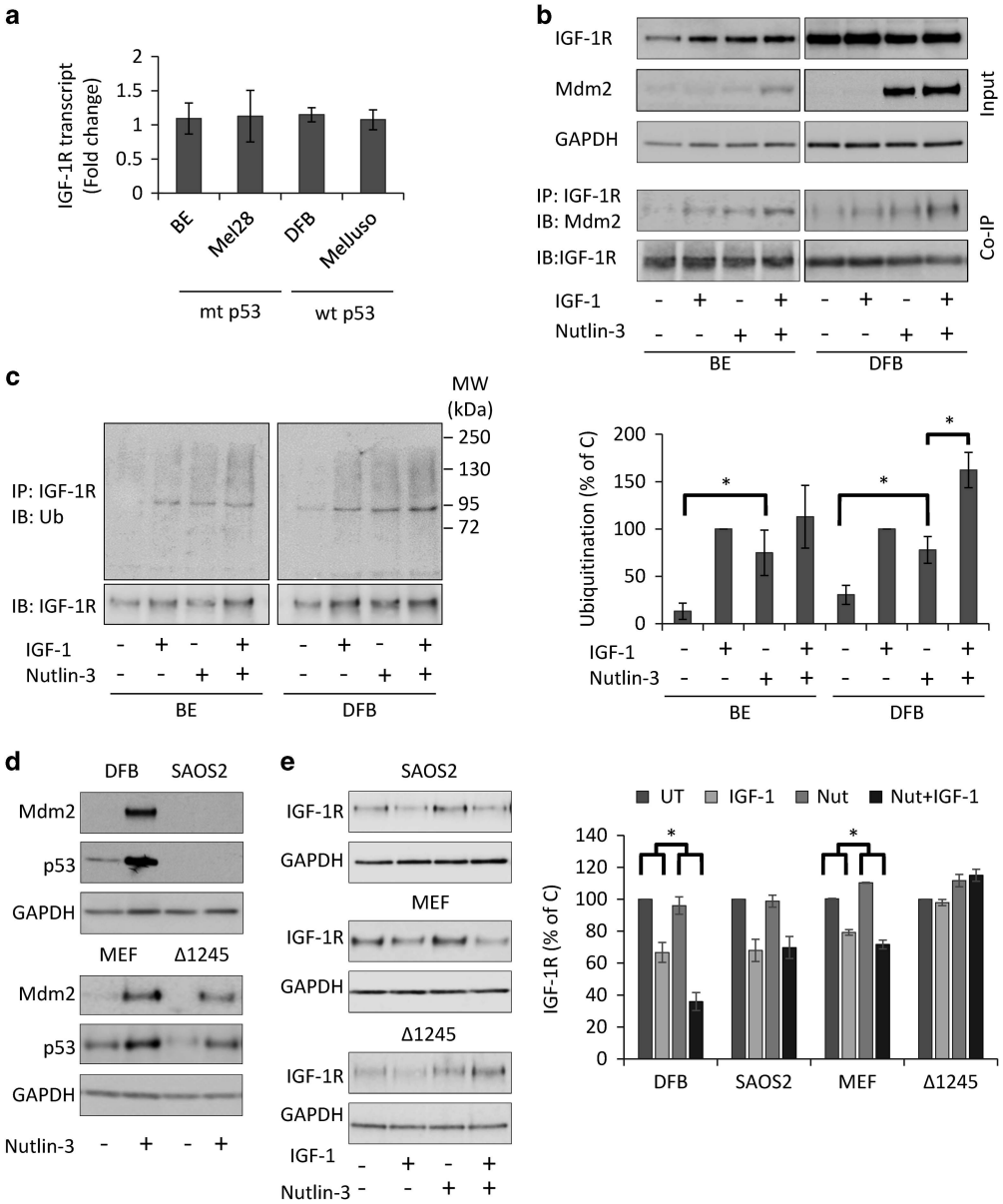

Figure 4. Mechanism of Nutlin-3-dependent IGF-1R downregulation. (**a**) Effect of Nutlin-3 on p53-induced IGF-1R transcription. Cells incubated in growth medium were treated with 1 μM Nutlin-3 for 12 h. RNA was isolated and the IGF-1R transcript level was quantified by qPCR, normalized to GAPDH transcripts levels and are displayed as fold change compared with their untreated controls. Data represent the mean ± s.e.m. from three independent experiments. (**b** and **c**) Effect of Nutlin-3 on Mdm2-dependent IGF-1R ubiquitination. Cells treated with either dimethyl sulfoxide (DMSO) or 1 μM Nutlin-3 in serum-free media for 8 h were stimulated or not with IGF-1 (50 ng/ml) for 10 min. IGF-1R, Mdm2 and GAPDH levels in the total protein lysates before IP were analyzed by WB (**b**). IGF-1R was immunoprecipitated and analyzed by WB (IB) for associated Mdm2 (**b**) or ubiquitination (Ub) (**c**) with IGF-1R as a loading control. Molecular weight markers in kDa are indicated to the right of the panel. IGF-1R ubiquitination signals were quantified by densitometry, normalized to total IGF-1R levels and displayed as a percentage of the ubiquitinated IGF-1R in the ligand-stimulated control cells. Data correspond to the mean ± s.e.m. from three independent experiments. Statistical analysis: $^*P < 0.05$. (**d** and **e**) Mdm2/IGF-1R interaction dependence of Nutlin-3-induced IGF-1R degradation. DFB, Mdm2/p53-SAOS2, MEF and MEF expressing truncated IGF-1R defective in binding Mdm2 (Δ1245) were analyzed for effects of Nutlin-3 on IGF-1R expression. Cells treated as indicated in serum-free media for 6 h and were stimulated or not with IGF-1 (50 ng/ml) for 24 h. The effects of Nutlin-3 treatment on p53 and Mdm2 accumulation were analyzed in total protein lysates by WB using GAPDH as a loading control. IGF-1R levels analyzed by WB were quantified by densitometry, normalized to GAPDH and expressed as a percentage of the IGF-1R levels in the control-treated cells (graph). Data correspond to the mean ± s.e.m. from three independent experiments. Statistical analysis: Nutlin-3-treated IGF-1-mediated IGF-1R degradation compared with IGF-1-mediated degradation alone: $^*P < 0.05$.

The ligand dependency of this association implies that agonist-induced receptor conformational changes stabilizes IGF-1R/Mdm2 interaction. As Mdm2 is an E3-ligase, the next logical step was to assess whether this direct association leads to increased IGF-1R ubiquitination as detected by WB after IP of the IGF-1R from the same samples as in Figure 4b. In untreated, serum-starved cells, there were very low levels of receptor ubiquitination, which increases dramatically after 10 min of IGF-1 (Figure 4c). Consistent with the pattern observed for Mdm2/IGF-1R association, Nutlin-3 alone increases the levels of IGF-1R ubiquitination, which further increases when cells were IGF-1 stimulated for 10 min (Figure 4c), confirmed by quantification across three experiments (Figure 4c, graph).

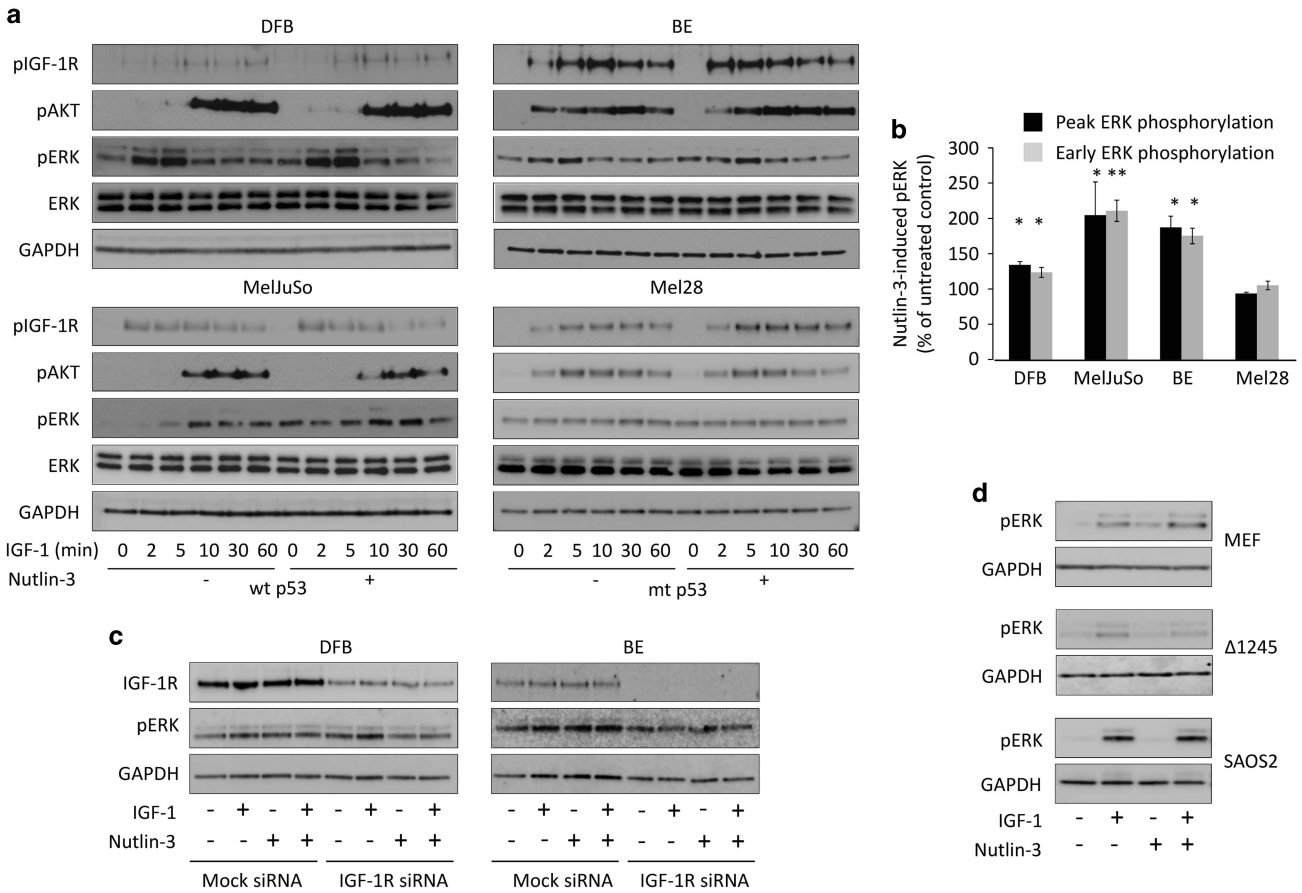

Figure 5. Effects of Nutlin-3 on IGF-1R-mediated signaling. (**a**) Serum-starved cells were treated or not with 1 μM Nutlin-3 for 8 h, followed by IGF-1 stimulation (50 ng/ml) for 0–60 min. Lysates were analyzed by WB for levels of phospho-IGF-1R (pIGF-1R), phospho-AKT (pAKT) and phospho-ERK (pERK), with GAPDH and total ERK (ERK) as a loading control. p53 status of the cell lines are indicated: wtp53 or mtp53. (**b**) Early (0 and 2 min) and peak (5 min for BE, DFB and Mel28 or 10 min for MelJuSo) ERK phosphorylation in cells treated without and with Nutlin-3 were quantified by densitometry from three independent experiments, normalized to GAPDH and displayed as a percentage of Nutlin-3 treated/untreated. Data correspond to the mean ± s.e.m. from three independent experiments. Statistical analysis: Nutlin-3-induced ERK phosphorylation compared with control cells: $*P < 0.05$, $**P < 0.01$. (**c** and **d**) Dependency of Nutlin-3-induced ERK phosphorylation on IGF-1R, Mdm2 and IGF-1R/Mdm2 interaction. BE and DFB cells transfected with IGF-1R siRNA, MEF WT, MEF IGF-1R Δ1245 and SAOS2 p53-/Mdm2- were treated as in panel (**a**) and stimulated with 50 ng/ml IGF-1 as indicated. Protein lysates were analyzed by WB for IGF-1R for transfection efficiency (**c**), pERK and GAPDH (**c** and **d**).

Having shown that Nutlin-3 treatment results in Mdm2 reassignment, decreased p53 degradation, enhanced Mdm2/IGF-1R association and subsequent receptor ubiquitination, we next asked whether there is a causative relationship between this process and receptor degradation. We used two different experimental systems: one without Mdm2/p53 loop and one expressing only IGF-1R deficient in binding Mdm2: (i) osteosarcoma SAOS2 cells, which lack Mdm2 and p53 loop and (ii) mouse embryonic fibroblast (MEF) cells knockout for IGF-1R and stably transfected with a C-terminal truncated IGF-1R (Δ1245)[51] alongside the equivalent MEF cells expressing full-length IGF-1R. The C-terminal truncated IGF-1R is unable to bind to β-arrestin, the adaptor protein directing the Mdm2-mediated IGF-1R ubiquitination.[42] In SAOS2 cells, we confirmed that Nutlin-3 treatment induced neither p53 nor Mdm2 accumulation, while both were increased in MEF WT, MEFΔ1245 and control DFB cell lines (Figure 4d). In SAOS2, ligand-induced IGF-1R degradation was unchanged with Nutlin-3 treatment (Figure 4e) indicating that either p53 or Mdm2 are essential for Nutlin-3-enhanced IGF-1R degradation. Likewise, in Δ1245 cells, with functional p53/Mdm2 but an IGF-1R defective in recruiting Mdm-2, not only did Nutlin-3 fail to induce degradation but instead also demonstrated a slight increase in IGF-1R. In contrast, the full-length IGF-1R in the MEF cells was degraded following Nutlin-3 treatment (Figure 4e). Notably, in the absence of ligand, Nutlin-3 treatment appears protective for IGF-1R in MEF cells. Quantification from multiple experiments confirms the dependency of IGF-1R degradation on a functional receptor–Mdm2 interaction (Figure 4e, graph).

Taken together, these experiments establish Mdm2-mediated ubiquitination and degradation of the IGF-1R as the key mechanism controlling Nutlin-3-induced IGF-1R downregulation.

Effects of Nutlin-3 on IGF-1R-mediated signaling

The effect of Nutlin-3-induced Mdm2 recruitment to the IGF-1R: decreased levels of the receptor through ubiquitination and degradation is only evident after longer (12–24 h) IGF-1 stimulation, overshadowing any effects Nutlin-3 may have on IGF-1R-mediated short-term signaling. We therefore explored the possible effects of Nutlin-3-mediated IGF-1R ubiquitination on signaling by treating serum-starved cells with Nutlin-3 for 8 h and then stimulating them with IGF-1 for up to 60 min. The effects on IGF-1R tyrosine kinase activation and downstream signaling through IRS/PI3K/AKT and Ras/Raf/MEK/extracellular signal-regulated kinase (ERK) pathways were verified by WB detection of phosphorylated IGF-1R, AKT and ERK as well as glyceraldehyde 3-phosphate dehydrogenase (GAPDH) and total ERK as loading controls (Figure 5a). In untreated cells, upon ligand stimulation the IGF-1R was phosphorylated within 2 min, demonstrating an

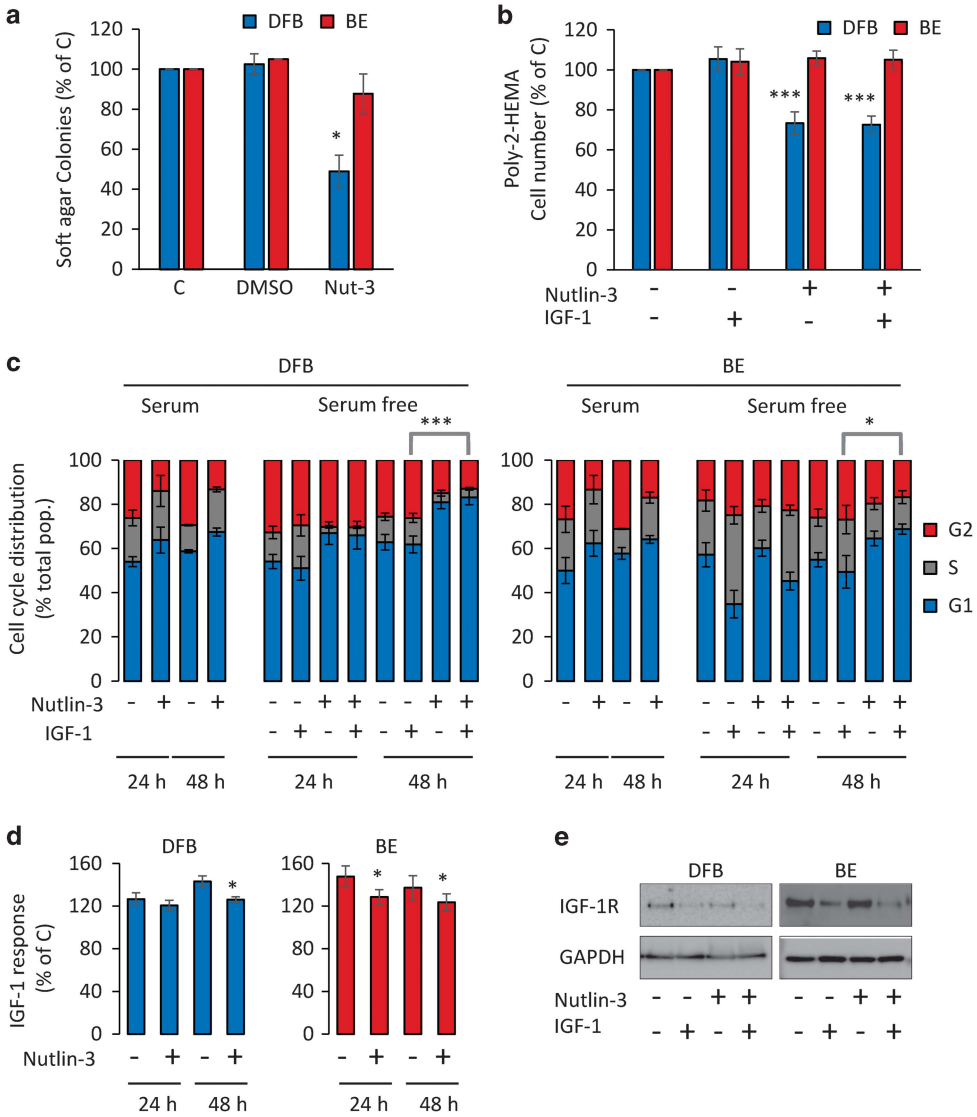

Figure 6. Effects of Nutlin-3 on IGF-1R modulated biological activities. (**a**) Effect of Nutlin-3 on growth in soft agar. BE and DFB cells were plated into 10% serum containing soft agar and treated with dimethyl sulfoxide (DMSO) or 1 μM Nutlin-3 for 14 days. The colonies were counted and the results from three independent experiments are displayed as mean ± s.e.m. relative to untreated control (C). (**b**) Effect of Nutlin-3 on cell viability in suspension. Cells plated into poly-2-HEMA-coated wells in serum-free medium were treated without and with 1 μM Nutlin-3 for 48 h in the presence or absence of IGF-1. The cell viability was measured by PrestoBlue reagent and displayed as a percentage of untreated controls. Data correspond to the mean ± s.e.m. from three independent experiments. (**c** and **d**) Effect of Nutlin-3 on cell cycle distribution and IGF-1-dependent cell viability. Cells growing in monolayer, treated as indicated, were analyzed for cell cycle distribution (G1, S and G2/M) (**c**) or cell viability (**d**). Results from three independent experiments are displayed as mean ± s.e.m., percentage of total cell population (**c**) or as mean ± s.e.m. relative to untreated cells (**d**). The levels of Nutlin-3-mediated IGF-1R degradation at 48 h were quantified in parallel samples by WB using GAPDH as a loading control (**e**). Statistical analysis: Nutlin-3-treated cells compared with control-treated cells: $^{*}P < 0.05$, $^{***}P < 0.001$.

increase in its kinase activity. Subsequently, both main signaling pathways were triggered as demonstrated by ERK and AKT phosphorylation (Figure 5a). Autophosphorylation of the IGF-1R in Nutlin-3-treated cells was unchanged compared with the equivalent untreated cells, suggesting that all cells still express functional IGF-1R after 8 h of Nutlin-3 treatment. This translated into comparable signaling through the PI3K/AKT pathway. Intriguingly, Nutlin-3 treatment caused an earlier and increased phosphorylation of ERK compared with untreated cells, as quantified from multiple experiments (Figure 5b). Notably, ERK activation was observed at time 0, in the absence of ligand stimulation in all cell lines except Mel28, which has high basal levels of phosphorylated ERK (Figures 5a and b).

ERK activation levels evident at time 0 in the Nutlin-3 treatment groups is potentially dependent on Mdm2-mediated IGF-1R ubiquitination. We verified this dependency by repeating the experiment while suppressing IGF-1R expression with specific small interfering RNA (siRNA). Efficiency of IGF-1R depletion was confirmed by WB (Figure 5c). In mock-transfected cells, Nutlin-3 treatment alone resulted in clear ERK activation similar to that obtained by 2 min of stimulation with IGF-1 (Figure 5c). Depletion of IGF-1R led to a substantial inhibition of the Nutlin-3-induced ERK phosphorylation with or without IGF-1 stimulation with the latter being completely abolished. Further confirming IGF-1R/Mdm2 interaction dependency, Nutlin-3 failed to activate the ERK phosphorylation in the absence of increased Mdm2 (SAOS2) or with a truncated IGF-1R (Δ1245) but did activate it in the MEF cells with full-length IGF-1R (Figure 5d).

Taken together, these experiments demonstrate the partial agonistic properties of Nutlin-3 for the MAPK pathway, mediated by Mdm2 through IGF-1R ubiquitination.

Effects of Nutlin-3 on IGF-1R-modulated biological activities

So far, our results demonstrate that Nutlin-3 affects the overall level, ubiquitination status, degradation and signaling dynamics of the IGF-1R. In particular, Nutlin-3 synergizes with IGF-1 in promoting IGF-1R ubiquitination and degradation, while enhancing MAPK signaling activation. The longer-term effect of receptor degradation competes with and eventually outweighs the short-term effect of increased ERK activation, so we next investigated how these seemingly counteracting effects alter IGF-1R cancer relevant bioactivities.

We first investigated how 1 μM of Nutlin-3 affects the tumorigenic potential of wtp53 DFB cells and mtp53 BE melanoma cells, as indicated by their ability to grow in anchorage-independent conditions, measured by colony formation in soft agar. Nutlin-3 inhibited the wtp53 DFB cell growth by 50%, whereas the mtp53 BE cell growth was inhibited by only 15% (Figure 6a).

Although the colony-formation assay provides evidence regarding the growth-suppressive effects of Nutlin-3 in the absence of matrix-induced cell survival signaling, it cannot fully determine the extent of IGF-1R contribution, as colony growth must be supported by full serum conditions. To specifically measure the effects of Nutlin-3 on IGF-1-mediated cell growth in anchorage-independent conditions, we used poly-2-hydroxyethylmethacrylate (poly-2-HEMA)-coated cell culture plates to prevent cell adhesion in a serum-free-based assay. After 48 h, IGF-1 alone had marginally increased cell proliferation in both cell lines, while 1 μM Nutlin-3 decreases cell number in the wtp53 cells irrespective of ligand stimulation (Figure 6b).

We next tested the IGF-1-dependent effects of Nutlin-3 on proliferation in an even less severe, adherent environment. Serum-starved cells were treated with and without Nutlin-3 and stimulated with and without IGF-1 for 24 and 48 h. Control and treated cells were analyzed for total cell number, and equivalent cell samples were analyzed by fluorescence-activated cell sorter (FACS) for cell cycle phase distribution (Figures 6c and d). Without serum, Nutlin-3 increases by 10–20% the total number of cells while decreasing their responsiveness to IGF-1 (Figures 6c and d). This effect is not only enhanced over time and is more evident in the wtp53 DFB cells but also occurs to a lesser extent in the mtp53 BE cells. The same pattern was displayed by the wtp53 MelJuSo, whereas mtp53 Mel28 were not affected (data not shown). Together, the proliferation data indicate a seemingly paradoxical behavior: Nutlin-3 treatment increases the total number of the cells in all cell lines (more evident in mtp53 cells) yet decreases the proportion in the proliferative phases (more evident in the

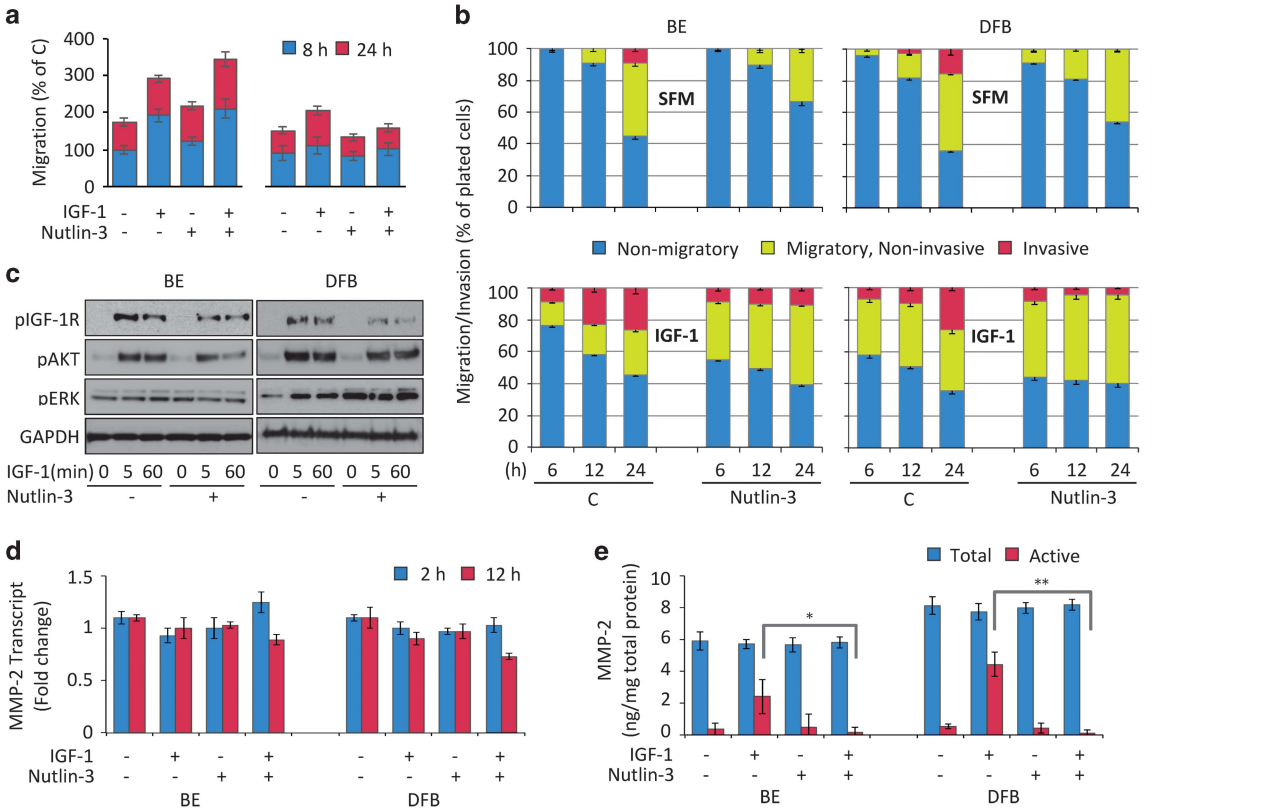

Figure 7. Effect of Nutlin-3 on IGF-1R-dependent melanoma migration and invasion. (**a**) Effect of Nutlin-3 on wound closure migration. A wound made in confluent monolayer of melanoma cells was treated with or without 1 μM Nutlin-3 for 8 h followed by IGF-1 stimulation for the indicated times. The rates of wound closure migration are displayed relative to the untreated cells control (C) as the mean ± s.e.m. from three independent experiments. (**b**–**e**) Effect of Nutlin-3-induced unbalanced IGF-1R signaling on migratory and invasive phenotype of the melanoma cells. Cells were treated with or without 1 μM Nutlin-3 for 12 h in serum-containing media to initiate IGF-1R downregulation. The Nutlin-3 effect on unbalanced response to IGF-1 was verified by WB testing the levels of p-IGF-1R, p-AKT, p-ERK and GAPDH as a loading control in lysates from the cells that were serum starved for 3 h before IGF-1 stimulation (**c**). Parallel samples pretreated with Nutlin-3 were fluorescently labeled with Dilc12 and then plated on the top of the transwell migration chambers, without (migration) or with (invasion) a layer of 5% Matrigel using 15% serum as a chemoattractant in the lower chamber and stimulated or not with IGF-1 in the top chamber. Bottom fluorescence of migrated/invaded cells was read at 6, 12 and 24 h time points and displayed as a percentage of the total number of the cells plated on the top chamber at time 0 (**b**). Cells treated as in panels (**b** and **c**) were used to evaluate the effects of Nutlin-3 on MMP-2 transcript expression by qRT-PCR (**d**) and to measure total and endogenously activated MMP-2 levels secreted in the culture media by enzyme-linked immunosorbent assay (**e**). MMP-2 transcript levels are normalized to GAPDH and displayed as a mean fold change ± s.e.m. relative to an untreated control (**d**). MMP-2 protein levels in the conditioned media are normalized to the total protein concentration in the cell lysates (ng/mg) and displayed as the mean of the absolute values ± s.e.m. (**e**). Statistical analysis: Nutlin-3-treated cells compared with control-treated cells: $^{*}P < 0.05$, $^{***}P < 0.001$.

wtp53). When compared with the IGF-1 alone conditions, Nutlin-3 decreases or completely abolishes the response to IGF-1 in wtp53 and mtp53 cells, respectively. An extended (48 h) Nutlin-3 treatment further decreases the proportion of proliferating cells in all cell lines and completely abolishes the responsiveness to IGF-1, as demonstrated both by the cell cycle analysis and the cell viability assay (Figures 6c and d). The reduction in IGF-1R was still sustained at this longer time point of 48 h treatment, as confirmed by WB analysis (Figure 6e).

Effects of Nutlin-3 treatment on IGF-1R-dependent melanoma migration and invasion

IGF-1R is a master regulator of the mechanisms controlling migration and invasion, essential components of the metastatic behavior. Hence, we next investigated the effect of Nutlin-3 treatment on the migratory phenotype of melanoma cells. As a pilot experimental approach, we used a monolayer wound-healing assay to evaluate the effects of Nutlin-3 on IGF-1-induced cell migration. In both wtp53 and mtp53 cell lines, 24 h of IGF-1 increases migration by around 50% (Figure 7a). Nutlin-3 treatment slightly increases this effect in the mtp53 BE cells, while decreasing it in the wtp53 cells. Notably, the wound-healing assay suggests that migration was preferentially inhibited towards the end of the experiment rather than during the first 8 h (Figure 7a), which coincides with the time frame of the Nutlin-3-induced early ERK activation at the expense of IGF-1R degradation. To confirm this behavior and extend our investigation into analyzing invasion and its dependency on IGF-1R expression and signaling, we employed a modified Transwell chamber assay allowing real-time analysis by fluorescent detection of prelabeled cells. The concurrent downregulation/signaling dual outcome was exposed by initiating IGF-1R depletion with Nutlin-3 treatment for 12 h serum (as in Figure 2c), followed by a 3 h serum starvation before testing receptor response to IGF-1. In both BE and DFB cell lines, IGF-1 induces receptor phosphorylation and balanced signaling through the ERK and AKT pathways, yet in the Nutlin-3-treated cells, the levels of IGF-1R and AKT phosphorylation after 5 or 60 min stimulation were considerably lower compared with untreated, indicating a reduction in IGF-1R at the cell surface (Figure 7c). On the other hand, the IGF-1R signaling was selectively directed toward MAPK pathways in Nutlin-3-treated cells as ERK was hyperphosphorylated, even in the absence of the ligand. We tested the effect of this unbalanced IGF-1R signaling on migratory and invasive phenotype of the melanoma cells. Fluorescently labeled cells, pretreated with Nutlin-3 as in Figure 7c for 12 h, were plated in the top chamber with IGF-1 as a stimulus, and 15% serum as a chemoattractant in the lower chamber. As a negative control, serum-free media was used in the lower chamber with $< 2\%$ of the cells demonstrating migration (data not shown). In the absence of treatment, the cells migrate through the membrane toward the serum in a time-dependent manner (Figure 7b, top panel). This is greatly enhanced by IGF-1 stimulation (Figure 7b, lower panel) especially during the first 12 h. In conditions with Nutlin-3 pretreatment unbalanced IGF-1R signaling, the initial (6 h) migratory phenotype of both melanoma cell lines was slightly enhanced; however, this lead diminishes over time and by the end of the experiment the cell migration kinetics of the Nutlin-3-treated cells is much slower than in the control group (Figure 7b, top panel). IGF-1 stimulation amplified the differences between Nutlin-3-treated cells and their control, with enhanced early migratory potential that is reversed by the end of the experiment in both cell lines (Figure 7b, lower panel). In mtp53 cells, the boost in migration occurs earlier and lasts longer than in wtp53 cells. By adding Matrigel—a reconstituted basement membrane—we were able to study the effect of Nutlin-3 treatment on the invasive potential. In the absence of IGF-1 stimulation, about 15–20% of the migrating cells were able to degrade and pass through the basement membrane after 24 h and this process was completely blocked by Nutlin-3 pretreatment (Figure 7b, top panel). IGF-1 stimulation doubled the invasive potential of the control group, with 40% of the migrating cells actively invading the basement membrane by 24 h (Figure 7b, lower panel). Intriguingly, although Nutlin-3 increases the early migratory phenotype, this behavior did not translate into an increased invasive phenotype, and the overall IGF-1-mediated invasion of both cells lines was completely inhibited by Nutlin-3 treatment. As IGF-1R was previously demonstrated to control the invasive phenotype through positive regulation of matrix metalloproteinase type 2 (MMP-2),[52,53] we investigated the effect of Nutlin-3 on IGF-1R-mediated expression and activation of MMP-2. We measured the MMP-2 transcript levels in the cells by qRT-PCR, and both the active and pro-MMP-2 secreted protein levels in the cell-conditioned media. The cells were treated or not with Nutlin-3 for 12 h in serum culture conditions to initiate IGF-1R parallel downregulation/signaling (as in Figures 7b and c). This was followed by serum-free incubation in the presence or absence of IGF-1, and culture media or RNA samples were collected at various time intervals. The MMP-2 RNA levels (Figure 7d) as well as the levels of total secreted MMP-2 (active and inactive; Figure 7e) were essentially unchanged by Nutlin-3 or IGF-1 treatment. On the other hand, in line with the observed enhanced invasive potential, in the control cells stimulated with IGF-1 approximately half of the total secreted MMP-2 was activated in both cell lines (Figure 7e) compared with activation of $< 10\%$ of secreted in untreated cells. In the cells pretreated with Nutlin-3, IGF-1-mediated MMP-2 activation was completely blocked, to below unstimulated levels (Figure 7e). This Nutlin-3-mediated decrease in IGF-1-dependent invasion through MMP-2 is controlled by a posttranscriptional mechanism, as the MMP-2 transcript levels were unmodified in the same conditions (Figure 7d).

Altogether these results demonstrate a dual effect of Nutlin-3 on IGF-1R-mediated bioactivities: (i) a modest inhibition of cell proliferation, that manifests itself more in wtp53 cells and at later time points; and (ii) biphasic effects on the migratory phenotype, with an early increase and late decrease in the number of migratory cells, more evident in mtp53 cells, while the invasiveness decreased following Nutlin-3 treatment regardless of the p53 status by reduced IGF-1-mediated MMP-2 activation.

DISCUSSION

The malignant phenotype is defined by orchestrated interactions between loss of tumor-suppressor mechanisms and gain of tumor-promoting signaling.[54] Probably the best-known feedback system in cancer pathogenesis is represented by the p53/Mdm2 interaction. Based on its ability to inactivate the 'good cop', p53 tumor suppressor, the classical paradigm describes Mdm2 as an oncogene and therapeutic strategies developed during the past decades specifically aimed to rescue p53 functions by antagonizing its natural inhibitor. Studies in several cancer types in which p53 is functionally inactivated demonstrated that p53 protein and activity levels are strongly induced by Nutlin-3. Yet, the outcome of Nutlin-3 treatment on Mdm2 expression and function has not been investigated. Hence, as the first key finding, the present study reveals that p53-released Mdm2 is functionally active toward the IGF-1R, another major cancer-relevant substrate. Three lines of evidence support this conclusion: first, we demonstrated that Nutlin-3-mediated IGF-1R degradation was dependent on the ligand-induced conformational changes; second, by co-IP we confirmed that Nutlin-3 induced IGF-1R/Mdm2 association and subsequent receptor ubiquitination, and finally, we established that Nutlin-3-induced IGF-1R degradation is prevented when Mdm2/IGF-1R interaction is inhibited (C-truncated IGF-1R) or Mdm2/p53 regulatory loop is absent (SAOS cells).

As IGF-1R inhibition at the transcriptional level is one critical mechanism by which p53 exerts its tumor-suppressor function, a key question was whether the identified IGF-1R downregulation was mediated by Mdm2 at the protein level or transcriptionally by Nutlin-3-reactivated p53. Our data support the first scenario as qPCR revealed no changes of the IGF-1R mRNA level following Nutlin-3 treatment. In addition, Nutlin-3-mediated receptor downregulation was demonstrated to be dependent on receptor conformation (ligand induced) as well as on a functional IGF-1R/Mdm2 interaction. It should be noted here, that in the absence of the ligand, Nutlin-3 seems to slightly enhance the expression of the IGF-1R in melanoma cells (Figure 3a) and more evident in MEF cells (Figures 4d and e). This suggests that, without ligand, ubiquitination levels do not reach the threshold required for targeting the receptor to the degradation pathways and instead drives receptor recycling, protecting its overall expression.[16]

The second key finding of the present report is the identification of the agonistic properties of Nutlin-3, demonstrated to activate ERK signaling as a result of IGF-1R ubiquitination. Thus, in addition to receptor degradation, Nutlin-3 triggers IGF-1R-dependent activation of the MAPK/ERK signaling pathway even in the absence of ligand stimulation. These results were confirmed both in mtp53- and wtp53-expressing cells and were demonstrated to be dependent on Mdm2/IGF-1R interaction.

It has been postulated that non-cancerous cell proliferation depends on prolonged exposure to mitogens that could be separated into a distinctive two-pulse scenario: a first signaling wave that includes ERK as a priming process, driving cells into early G1, which parallel a p53-regulated restraining response.[55] A second pulse of mitogens generates PI3K signals that release the p53 constraint as well as generating a sustained MAPK signal, helping the cells to complete the cell cycle.[55] In the context of cancer, as the p53-constraining mechanism is inactivated, the cells would become responsive to subthreshold exposures to growth factors, thus creating growth advantage over the normal cells. In the case of melanoma, in which MAPK pathway is constitutively activated by Ras/BRAF mutation, the control mechanism represented by MAPK threshold is easily surpassed.

This scenario is consistent with the biphasic biological effects observed following Nutlin-3 treatment as well as with the downregulation and signaling activation dual role of Mdm2 on IGF-1R. Exposure to low doses of Nutlin-3 initiates the first signaling wave, stimulating the cells to enter into the cell cycle, thus explaining the initial increase in cell proliferation. As Nutlin-3 also activates the p53-restraining response, the effect is revealed in wtp53-expressing cells. On the other hand, this MAPK activation is carried out at the cost of IGF-1R downregulation and unbalanced MAPK/PI3K signaling, which in turn will affect the second signaling wave and prevent entry into a new proliferative cycle. As IGF-1R is depleted by Nutlin-3 treatment, the effects of unbalanced MAPK/PI3K on cell viability are revealed following 48 h Nutlin-3 treatment.

An intriguing finding of the present study is the effect of IGF-1R downregulation by Nutlin-3 treatment on the major mechanisms controlling melanoma metastasis. Although increasing the migratory capacity of the melanoma cells, Nutlin-3 treatment completely abolishes their invasive potential. Although migration is dependent mostly on the MAPK pathway, it is not surprising that Nutlin-3-induced ERK activation promotes cell mobility. On the other hand, invasive cells required MAPK/PI3K balanced activation and responsive IGF-1R to control MMP-2 activation through the membrane-type MMPs (MT1-MMP).[56–59] The latter pathways were both crippled by Nutlin-3-induced IGF-1R downregulation.

Acting as a ubiquitin ligase for both p53 and IGF-1R, Mdm2 is a master regulator of the pathways converging in stress-induced survival: p53 accumulation halts the cell cycle, allowing for adequate DNA repair, while an Mdm-2-activated IGF-1R allows for cell survival and a return to the cell cycle once appropriate.[15] UV-irradiated human melanocytes (harboring wtp53) increase their levels of IGF-1R and cell survival as a result of Mdm2 sequestration by accumulated p53. Conversely, in conditions where Mdm2 was prevented from interacting with p53, IGF-1R expression was drastically decreased along with cell viability.[13] Within the same scenario, preventing p53–Mdm2 interaction, Nutlin-3 amplifies IGF-1R–Mdm2 association, unbalancing its signaling.

As both the p53 and IGF-1R pathways are being targeted by cancer therapeutics in studies and trials,[60,61] it is crucial to understand how targeting of one might affect signaling through the other. We demonstrated that disruption of the Mdm2–p53 interaction by Nutlin-3 treatment in melanoma, allowing Mdm2 accumulation, will have subsequent effects on the Mdm2-dependent ubiquitination of IGF-1R and will therefore affect IGF-1 signaling dynamics and alter cancer-relevant cell behaviors: proliferation, migration, and invasion.

Taken together, our results provide fundamental insights into Mdm-2 activation in melanoma cells, which result in destabilization of the p53/Mdm2/IGF-1R axis with receptor downregulation and MAPK/PI3K unbalanced signal activation. These mechanisms can be targeted through small-molecule inhibitors and potentially deployed for therapeutic gain.

MATERIALS AND METHODS

Cell lines and materials

Mel28 and MelJuSo were obtained from ATCC (Manassas, VA, USA) and BE and DFB were obtained from Dr Rolf Kiessling, KI, Stockholm, Sweden.[62] BE contains a hot-spot mutation in the p53 codon 248 and Mel28 contains a mutation in codon 145.[13,63,64] Sequencing of all melanoma cell lines confirmed their previously reported p53 status (data not shown).[13,65] BE and DFB were grown in RPMI supplemented with 10% (v/v) fetal bovine serum (FBS), MelJuSo in Dulbecco's modified Eagle's medium supplemented with 10% (v/v) FBS and Mel28 in Minimum Essential Medium supplemented with 10% (v/v) FBS. All melanoma cell lines were sequenced to confirm their known p53 status. MEF and Δ1245 (IGF-1R null background cells stably transfected with IGF-1R with C-terminal tail truncation at residue 1245) were obtained from Dr Renato Baserga, Thomas Jefferson University, Philadelphia, PA, USA[66] and grown in Dulbecco's modified Eagle's medium supplemented with 10% FBS and 100 μg/ml G418. SAOS2 (human osteosarcoma cell line) was obtained from ATCC and grown in Iscove's Modified Dulbecco's Medium supplemented with 10% FBS. All human cell lines were verified for authenticity by short tandem repeat profiling. Mouse cell lines were authenticated by examination of morphology, growth characteristics and the expression of truncated IGF-1R. All cell lines were tested for mycoplasma contamination regularly.

Nutlin-3 was dissolved in dimethyl sulfoxide at 2 mM and diluted in cell medium prior to use. Recombinant human IGF-1 was dissolved in 2% (w/v) bovine serum albumin (BSA) at a concentration of 50 mg/ml. All materials were from Sigma Aldrich Ltd. (St Louis, MO, USA) unless otherwise stated.

siRNA transfection

Cells were reverse transfected, with siRNA against IGF-1R (Ambion, Life Technologies Göteborg, Sweden, s7211, 5′-GCAUGGUAGCCGAAGAUUUtt-3′) using RNAiMAX (Life Technologies) according to the manufacturer's instructions. The reverse transfection procedure involved preparing diluted transfection reagent and siRNA in the cell culture vessel and adding single-cell suspensions of the cell lines on top and allowing the cells to attach.

SDS-PAGE (sodium dodecyl sulfate-polyacrylamide gel electrophoresis) and western transfer analysis

Cells were washed with phosphate-buffered saline (PBS), lysed in LDS sample buffer supplemented with 5% (v/v) beta-mercaptoethanol and boiled at 95 °C for 10 min prior to loading onto a 4–12% Bis-Tris precast gradient polyacrylamide gel (Invitrogen, Carlsbad, CA, USA) and separated by electrophoresis at 120 mA for 1 h. Proteins were transferred to nitrocellulose membrane by electrophoresis at 100 V for 1 h. Membranes were blocked with 5% (w/v) BSA or milk in Tris-buffered saline (TBS) with

0.1% (v/v) Tween 20 (TBST) and incubated with primary antibody overnight at 4 °C in BSA or milk TBST. Primary antibodies for IGF-1R (no. 3027, 1:2000 in BSA), phospho-ERK (no. 9101, 1:2000 in BSA), phospho-AKT (no. 4060, 1:2000 in BSA) and phospho-IGF-1R (no. 3021, 1:2000 in BSA) were from Cell Signaling Technologies (Danvers, MA, USA). Primary antibodies for p53 (sc-126, 1:1000 in milk), Mdm2 (sc-5304, 1:500 in milk), ubiquitin (P4D1, sc-8017, 1:1000 in milk) and GAPDH (sc-25778, 1:4000 in milk) were from Santa Cruz Biotechnologies (Santa Cruz, CA, USA). Following TBST washes, membranes were incubated with the appropriate horseradish peroxidase-coupled secondary antibody from Pierce (Rockford, IL, USA) at 1:2000 in milk TBST at room temperature for 1 h. Membranes were incubated with ECL substrate (Pierce) for 1 min and exposed to film or imaged using the Odyssey system (Li-cor, Lincoln, NE, USA). Data shown as images are from one representative experiment of at least three experiments.

Densitometric analysis of western transfer analysis

Western transfer analysis bands were quantified using the ImageJ program (http://rsbweb.nih.gov/ij/), subtracting the background level.

Cell viability assay

Cells in complete medium in 96-well plates were allowed to attach. Each condition was performed in triplicate and an untreated control was included. Cells were incubated with PrestoBlue (Life Technologies) reagent for 30 min and the fluorescence from excitation at 560 nm and emission at 590 nm was measured. A standard curve was used to interpolate fluorescence to cell number.

IGF-1R immunoprecipitation

Following treatment, cells cultured in six-well plates were washed with PBS, lysed in 500 µl lysis buffer (110 mM KOAc, 0.5% (v/v) Triton X-100, 100 mM NaCl, buffering salts pH 7.4) and the protein concentration was determined by bicinchoninic acid assay (Pierce). Dynabeads protein G (10 µl; Invitrogen) and 1 µg antibody were added to 500 µg of protein. After overnight incubation at 4 °C on a rotator platform, the immunoprecipitate/Dynabeads were collected on a magnetic rack, the supernatant discarded and the beads were washed with lysis buffer and dissolved in the SDS-PAGE sample buffer.

qRT-PCR for IGF-1R, GAPDH and MMP-2

qRT-PCR for the IGF-1R/GAPDH experiment (Figure 4) was performed using the GeneJet RNA Purification Kit (Fermantas, St Leon-Rot, Germany) and Sigma synthesized primers: GAPDH: F 5′-GGGAAGCTTGTCATCAATGG-3′, R 5′-CTCCATGGTGGTGAAGACG-3′, IGF-1R: F 5′-TGAGAAAGGGGAATTTCATCC-3′, R 5′-ATAGTCGTTGCGGATGTCG-3′, with a SYBR Green/ROX qPCR Master Mix (Fermentas, Thermo Fisher Scientific, Göteborg, Sweden) as previously described.[40] For the MMP-2 experiment (Figure 7), RNA extraction was carried out using a PureLink RNA Kit (Ambion) according to the manufacturer's instructions. A 1 µg aliquot of RNA was treated in 1 µl 10X DNase I Reaction Buffer, 1 µl DNase I, Amp Grade (Invitrogen) for 15 min at room temperature. The DNase was inactivated by addition of 1 µl of 25 mM EDTA solution to the reaction mixture. The mixture was heated for 10 min at 65 °C. MMP-2 gene expression was measured using FAM-labeled TaqMan assay (RNA to ct One Step Kit, Applied Biosystems, Göteborg, Sweden) and specific human probes (Hs01548727_m1) for MMP-2. Real-time qPCRs were performed with the StepOne Plus Real-Time PCR System (Applied Biosystems).

PCR amplifications were performed in a total volume of 20 µl Master Mix, containing 5 µl sample, TaqMan RT-PCR Mix (2×), TaqMan RT Enzyme Mix (40×), TaqMan Gene Expression Assay (Applied Biosystems) and H_2O. Predeveloped GAPDH endogenous control reagents were used as control genes from the same samples. MicroAmp Optical 96-Well Reaction Plates and Optical Caps (Applied Biosystems) were used in reactions. Reaction conditions were as follows: 15 min at 48 °C and 10 min at 95 °C, followed by 40 cycles of 15 s at 95 °C and 1 min at 60 °C. Relative expression levels were determined by the ΔΔCт method.[67]

Cell cycle distribution analysis

Following treatment, cells were collected and centrifuged at 1500 r.p.m. for 4 min to pellet. The supernatant was discarded and the pellet was resuspended dropwise in 0.5 ml 4% formalin and fixed for >12 h. Following centrifugation at 1500 r.p.m. for 4 min, the pellet was resuspended dropwise in 0.5 ml of 95% ethanol and incubated for >1 h. Cells were rehydrated in water and treated with protease subtilisin Carlsberg for 1 h at 45 °C. Nuclei were then stained with 4,6-diamidino-2-phenylindole for 30 min before analysis by FACS.[68]

poly-2-HEMA growth assay

Tissue culture plate wells were coated with 200 µg/cm^2 of poly-2-HEMA solution dissolved in 95% ethanol and left to dry. Cells were plated and treated in the wells, and the cell viability was assayed.

Wound-healing assay

Cell monolayers at high confluency in 24-well plates were wounded with a p200 pipette tip and washed with PBS, and the serum-free medium was added. During treatment, wounds were photographed at 0, 8 and 24 h. Wound width at each time point was measured using ImageJ (http://rsbweb.nih.gov/ij/) and the extent of movement at each wound edge was calculated (average wound width at 0 h − average wound width at 24 h)/2.

Colony-formation assay

Forty-eight-well plate wells were coated with 100 µl of molten 0.6% agar in growth medium and allowed to set. Cells were resuspended in molten 0.3% agar in growth medium at 40 000/ml, and 50 µl was added to each well. Complete growth medium was added to the well, and the cells were incubated for 14 days, changing the growth medium every 3 days. The colonies were stained using a 0.005% (w/v) crystal violet stain for 1 h, and excess stain was removed with PBS washes. The wells were photographed, and the colonies were counted using the Image J software.

Migration/invasion assay

The migratory/invasive potential of the cells was tested using BD BioCoat Tumor Invasion System (BD Biosciences-Europe, Oxford, UK) as previously described.[40] The system consists of a BD Falcon FluoroBlok 24-Multiwell Insert Plate with an 8-µm pore size PET membrane coated with Matrigel, for invasion, or uncoated for migration. Cells were stained with Dilc12 for 2 h and seeded at 5×10^4 cells in 500 µl of serum-free medium with IGF-1 (20 ng/ml) onto the apical chamber. In all, 500 µl of media containing 10% serum was added to the bottom chamber as chemoattractant. Equal seeding was verified by measuring the top fluorescence. The plates were incubated at 37 °C in a humidified 5% CO_2 atmosphere for 24 h. During incubation, the fluorescence of the invaded cells on the bottom side of the membrane was measured using a Tecan Infinite M1000 plate reader (Tecan Group Ltd, Männedorf, Switzerland) at 6-, 12- and 24-h time points. Data were converted, using a standard curve, to percentage of the total cells added to the top chamber at the start of the experiment. Each experiment was performed in triplicate.

MMP-2 enzyme-linked immunosorbent assay

MMP-2 activity was measured using the Amersham Biotrak Activity Assay System (GE Healthcare UK Ltd, Buckinghamshire, UK). Cells were plated, allowed to attach in complete growth media, washed with PBS and changed to serum-free media. As well as a serum-free media only control, one group received IGF-1 (50 ng/ml) and the third received IGF-1 (50 ng/ml) and Nutlin-3 (1 µM). Cells were incubated with their respective medias for 12 h, after which time the conditioned media was collected and cells discarded. Levels of active MMP-2 in the collected conditioned media were assayed by following the MMP-2 Biotrack Activity Assay manufacturer's protocol. Briefly; conditioned media was added to an anti-MMP-2-coated 96-well microplate to capture endogenous MMP-2. Following washing steps, MMP-2 levels are detected by way of a detection reagent and optical density 405-nm reading using a TECAN infinite M1000 plate reader (Tecan Group Ltd), and signal conversion using a standard curve of known MMP-2 concentration. Quantification of the total and endogenously active MMP-2 was performed by adding *p*-aminophenylmercuric acetate solution to obtain a 'Total MMP-2' for that sample.

Statistical analysis

Where indicated, data from a minimum of three independent experimental replicates of two conditions were compared using a two-tailed, unpaired *t*-test assuming equal variance. As part of the experimental design, before performing the experiment, a threshold value of $P=0.05$ was chosen for

testing the null hypothesis. The variances of the experimental groups that are being compared were not statistically different. Data expressed with error bars show mean ± s.e.m. from three independent biological experiments, unless otherwise stated. Significance is given as $*P < 0.05$, $**P < 0.01$, $***P < 0.005$.

CONFLICT OF INTEREST

The authors declare no conflict of interest.

ACKNOWLEDGEMENTS

We thank Professor Rolf Kiessling (CCK, KI) for the BE and DFB cell lines 62, to Juan Castro (CCK, KI) for FACS analysis and to Dr Cath Drummond and Dr Sonia Laín for helpful discussions. Research support was received from the Swedish Research Council, Swedish Cancer Society, The Swedish Childhood Cancer Foundation, Crown Princess Margareta's Foundation for the Visually Impaired, Welander Finsen Foundation, King Gustaf V Jubilee Foundation, Stockholm Cancer Society, Stockholm County and Karolinska Institute. This work was also supported by Grant-in-Aid of Scientific Research (S) no. 25221204, Core-to-core program from JSPS to S-IT group.

REFERENCES

1 Cummins DL, Cummins JM, Pantle H, Silverman MA, Leonard AL, Chanmugam A. Cutaneous malignant melanoma. *Mayo Clin Proc* 2006; **81**: 500–507.
2 Kanavy HE, Gerstenblith MR. Ultraviolet radiation and melanoma. *Semin Cutan Med Surg* 2011; **30**: 222–228.
3 Olivier M, Hollstein M, Hainaut P. TP53 mutations in human cancers: origins, consequences, and clinical use. *Csh Perspect Biol* 2010; **2**: a001008.
4 Mar VJ, Wong SQ, Li J, Scolyer RA, McLean C, Papenfuss AT *et al.* BRAF/NRAS wild-type melanomas have a high mutation load correlating with histologic and molecular signatures of UV damage. *Clin Cancer Res* 2013; **19**: 4589–4598.
5 Castresana JS, Rubio MP, Vazquez JJ, Idoate M, Sober AJ, Seizinger BR *et al.* Lack of allelic deletion and point mutation as mechanisms of p53 activation in human malignant melanoma. *Int J Cancer* 1993; **55**: 562–565.
6 Albino AP, Vidal MJ, McNutt NS, Shea CR, Prieto VG, Nanus DM *et al.* Mutation and expression of the p53 gene in human malignant melanoma. *Melanoma Res* 1993; **55**: 562–565.
7 Hocker T, Tsao H. Ultraviolet radiation and melanoma: a systematic review and analysis of reported sequence variants. *Hum Mutat* 2007; **28**: 578–588.
8 Lane D, Levine A. p53 Research: the past thirty years and the next thirty years. *Cold Spring Harb Perspect Biol* 2010; **2**: a000893.
9 Fuchs SY, Adler V, Buschmann T, Wu X, Ronai Z. Mdm2 association with p53 targets its ubiquitination. *Oncogene* 1998; **17**: 2543–2547.
10 Iwakuma T, Lozano G. MDM2, an introduction. *Mol Cancer Res* 2003; **1**: 993–1000.
11 Fakharzadeh SS, Trusko SP, George DL. Tumorigenic potential associated with enhanced expression of a gene that is amplified in a mouse-tumor cell-line. *EMBO J* 1991; **10**: 1565–1569.
12 Manfredi JJ. The Mdm2-p53 relationship evolves: Mdm2 swings both ways as an oncogene and a tumor suppressor. *Gene Dev* 2010; **24**: 1580–1589.
13 Girnita L, Girnita A, Brodin B, Xie Y, Nilsson G, Dricu A *et al.* Increased expression of insulin-like growth factor I receptor in malignant cells expressing aberrant p53: functional impact. *Cancer Res* 2000; **60**: 5278–5283.
14 Davenport RJ. Trashing a Longevity-Slasher p53 partner disposes of a protein that promotes aging. *Sci SAGE KE* 2003; **10**: 1126.
15 Girnita L, Girnita A, Larsson O. Mdm2-dependent ubiquitination and degradation of the insulin-like growth factor 1 receptor. *Proc Natl Acad Sci USA* 2003; **100**: 8247–8252.
16 Girnita L, Takahashi SI, Crudden C, Fukushima T, Worrall C, Furuta H *et al.* Chapter seven - when phosphorylation encounters ubiquitination: a balanced perspective on IGF-1R signaling. *Prog Mol Biol Transl Sci* 2016; **141**: 277–311.
17 Molhoek KR, Shada AL, Smolkin M, Chowbina S, Papin J, Brautigan DL *et al.* Comprehensive analysis of receptor tyrosine kinase activation in human melanomas reveals autocrine signaling through IGF-1R. *Melanoma Res* 2011; **21**: 274–284.
18 Karasic TB, Hei TK, Ivanov VN. Disruption of IGF-1R signaling increases TRAIL-induced apoptosis: a new potential therapy for the treatment of melanoma. *Exp Cell Res* 2010; **316**: 1994–2007.
19 Yeh AH, Bohula EA, Macaulay VM. Human melanoma cells expressing V600E B-RAF are susceptible to IGF1R targeting by small interfering RNAs. *Oncogene* 2006; **25**: 6574–6581.
20 Neudauer CL, McCarthy JB. Insulin-like growth factor I-stimulated melanoma cell migration requires phosphoinositide 3-kinase but not extracellular-regulated kinase activation. *Exp Cell Res* 2003; **286**: 128–137.
21 Economou MA, Andersson S, Vasilcanu D, All-Ericsson C, Menu E, Girnita A *et al.* Oral picropodophyllin (PPP) is well tolerated in vivo and inhibits IGF-1R expression and growth of uveal melanoma. *Invest Ophthalmol Vis Sci* 2008; **49**: 2337–2342.
22 Puzanov I, Lindsay CR, Goff L, Sosman J, Gilbert J, Berlin J *et al.* A phase I study of continuous oral dosing of OSI-906, a dual inhibitor of insulin-like growth factor-1 and insulin receptors, in patients with advanced solid tumors. *Clin Cancer Res* 2015; **21**: 701–711.
23 Mahadevan D, Sutton GR, Arteta-Bulos R, Bowden CJ, Miller PJE, Swart RE *et al.* Phase 1b study of safety, tolerability and efficacy of R1507, a monoclonal antibody to IGF-1R in combination with multiple standard oncology regimens in patients with advanced solid malignancies. *Cancer Chemother Pharm* 2014; **73**: 467–473.
24 Macaulay VM, Middleton MR, Protheroe AS, Tolcher A, Dieras V, Sessa C *et al.* Phase I study of humanized monoclonal antibody AVE1642 directed against the type 1 insulin-like growth factor receptor (IGF-1R), administered in combination with anticancer therapies to patients with advanced solid tumors. *Ann Oncol* 2013; **24**: 784–791.
25 Kanter-Lewensohn L, Dricu A, Wang M, Wejde J, Kiessling R, Larsson O. Expression of the insulin-like growth factor-1 receptor and its anti-apoptotic effect in malignant melanoma: a potential therapeutic target. *Melanoma Res* 1998; **8**: 389–397.
26 Vasilcanu D, Weng WH, Girnita A, Lui WO, Vasilcanu R, Axelson M *et al.* The insulin-like growth factor-1 receptor inhibitor PPP produces only very limited resistance in tumor cells exposed to long-term selection. *Oncogene* 2006; **25**: 3186–3195.
27 Zerp SF, van Elsas A, Peltenburg LT, Schrier PI. p53 mutations in human cutaneous melanoma correlate with sun exposure but are not always involved in melanomagenesis. *Br J Cancer* 1999; **79**: 921–926.
28 Box NF, Terzian T. The role of p53 in pigmentation, tanning and melanoma. *Pigment Cell Melanoma Res* 2008; **21**: 525–533.
29 Gasbarri A, Del Prete F, Girnita L, Martegani MP, Natali PG, Bartolazzi A. CD44s adhesive function spontaneous and PMA-inducible CD44 cleavage are regulated at post-translational level in cells of melanocytic lineage. *Melanoma Res* 2003; **13**: 325–337.
30 Klein C, Vassilev LT. Targeting the p53-MDM2 interaction to treat cancer. *Br J Cancer* 2004; **91**: 1415–1419.
31 Vassilev LT. Small-molecule antagonists of p53-MDM2 binding: research tools and potential therapeutics. *Cell Cycle* 2004; **3**: 419–421.
32 Vassilev LT, Vu BT, Graves B, Carvajal D, Podlaski F, Filipovic Z *et al.* In vivo activation of the p53 pathway by small-molecule antagonists of MDM2. *Science* 2004; **303**: 844–848.
33 Shangary S, Wang S. Small-molecule inhibitors of the MDM2-p53 protein-protein interaction to reactivate p53 function: a novel approach for cancer therapy. *Annu Rev Pharmacol Toxicol* 2009; **49**: 223–241.
34 van Leeuwen IM, Higgins M, Campbell J, Brown CJ, McCarthy AR, Pirrie L *et al.* Mechanism-specific signatures for small-molecule p53 activators. *Cell Cycle* 2011; **10**: 1590–1598.
35 Ji Z, Njauw CN, Taylor M, Neel V, Flaherty KT, Tsao H. p53 rescue through HDM2 antagonism suppresses melanoma growth and potentiates MEK inhibition. *J Invest Dermatol* 2012; **132**: 356–364.
36 Fahraeus R, Olivares-Illana V. MDM2's social network. *Oncogene* 2014; **33**: 4365–4376.
37 Girnita L, Worrall C, Takahashi S, Seregard S, Girnita A. Something old, something new and something borrowed: emerging paradigm of insulin-like growth factor type 1 receptor (IGF-1R) signaling regulation. *Cell Mol Life Sci* 2014; **71**: 2403–2427.
38 Crudden C, Ilic M, Suleymanova N, Worrall C, Girnita A, Girnita L. The dichotomy of the Insulin-like growth factor 1 receptor: RTK and GPCR: friend or foe for cancer treatment? *Growth Horm IGF Res* 2015; **25**: 2–12.
39 Zheng H, Shen H, Oprea I, Worrall C, Stefanescu R, Girnita A *et al.* beta-Arrestin-biased agonism as the central mechanism of action for insulin-like growth factor 1 receptor-targeting antibodies in Ewing's sarcoma. *Proc Natl Acad Sci USA* 2012; **109**: 20620–20625.
40 Zheng H, Worrall C, Shen H, Issad T, Seregard S, Girnita A *et al.* Selective recruitment of G protein-coupled receptor kinases (GRKs) controls signaling of the insulin-like growth factor 1 receptor. *Proc Natl Acad Sci USA* 2012; **109**: 7055–7060.
41 Sehat B, Andersson S, Girnita L, Larsson O. Identification of c-Cbl as a new ligase for insulin-like growth factor-I receptor with distinct roles from Mdm2 in receptor ubiquitination and endocytosis. *Cancer Res* 2008; **68**: 5669–5677.
42 Girnita L, Shenoy SK, Sehat B, Vasilcanu R, Girnita A, Lefkowitz RJ *et al.* {beta}-Arrestin is crucial for ubiquitination and down-regulation of the insulin-like growth factor-1 receptor by acting as adaptor for the MDM2 E3 ligase. *J Biol Chem* 2005; **280**: 24412–24419.
43 Girnita L, Shenoy SK, Sehat B, Vasilcanu R, Vasilcanu D, Girnita A *et al.* Beta-arrestin and Mdm2 mediate IGF-1 receptor-stimulated ERK activation and cell cycle progression. *J Biol Chem* 2007; **282**: 11329–11338.

44 Girnita A, Zheng H, Gronberg A, Girnita L, Stahle M. Identification of the cathelicidin peptide LL-37 as agonist for the type I insulin-like growth factor receptor. *Oncogene* 2012; **31**: 352–365.
45 Sehat B, Andersson S, Vasilcanu R, Girnita L, Larsson O. Role of ubiquitination in IGF-1 receptor signaling and degradation. *PLoS One* 2007; **2**: e340.
46 Economou MA, All-Ericsson C, Bykov V, Girnita L, Bartolazzi A, Larsson O *et al.* Receptors for the liver synthesized growth factors IGF-1 and HGF/SF in uveal melanoma: intercorrelation and prognostic implications. *Invest Ophthalmol Vis Sci* 2005; **46**: 4372–4375.
47 Werner H, Shalita-Chesner M, Abramovitch S, Idelman G, Shaharabani-Gargir L, Glaser T. Regulation of the insulin-like growth factor-I receptor gene by oncogenes and antioncogenes: implications in human cancer. *Mol Genet Metab* 2000; **71**: 315–320.
48 Webster NJ, Resnik JL, Reichart DB, Strauss B, Haas M, Seely BL. Repression of the insulin receptor promoter by the tumor suppressor gene product p53: a possible mechanism for receptor overexpression in breast cancer. *Cancer Res* 1996; **56**: 2781–2788.
49 Werner H, Sarfstein R. Transcriptional and epigenetic control of IGF1R gene expression: implications in metabolism and cancer. *Growth Horm IGF Res* 2014; **24**: 112–118.
50 Werner H, Karnieli E, Rauscher FJ, LeRoith D. Wild-type and mutant p53 differentially regulate transcription of the insulin-like growth factor I receptor gene. *Proc Natl Acad Sci USA* 1996; **93**: 8318–8323.
51 Hongo A, D'Ambrosio C, Miura M, Morrione A, Baserga R. Mutational analysis of the mitogenic and transforming activities of the insulin-like growth factor I receptor. *Oncogene* 1996; **12**: 1231–1238.
52 Girnita A, All-Ericsson C, Economou MA, Astrom K, Axelson M, Seregard S *et al.* The insulin-like growth factor-I receptor inhibitor picropodophyllin causes tumor regression and attenuates mechanisms involved in invasion of uveal melanoma cells. *Clin Cancer Res* 2006; **12**: 1383–1391.
53 Zhang D, Brodt P. Type 1 insulin-like growth factor regulates MT1-MMP synthesis and tumor invasion via PI 3-kinase/Akt signaling. *Oncogene* 2003; **22**: 974–982.
54 Hanahan D, Weinberg RA. Hallmarks of cancer: the next generation. *Cell* 2011; **144**: 646–674.
55 Zwang Y, Sas-Chen A, Drier Y, Shay T, Avraham R, Lauriola M *et al.* Two phases of mitogenic signaling unveil roles for p53 and EGR1 in elimination of inconsistent growth signals. *Mol Cell* 2011; **42**: 524–535.
56 Vasilcanu R, Vasilcanu D, Sehat B, Yin S, Girnita A, Axelson M *et al.* Insulin-like growth factor type-I receptor-dependent phosphorylation of extracellular signal-regulated kinase 1/2 but not Akt (protein kinase B) can be induced by picropodophyllin. *Mol Pharmacol* 2008; **73**: 930–939.
57 Zhang D, Samani AA, Brodt P. The role of the IGF-I receptor in the regulation of matrix metalloproteinases, tumor invasion and metastasis. *Horm Metab Res* 2003; **35**: 802–808.
58 Zhang DL, Bar-Eli M, Meloche S, Brodt P. Dual regulation of MMP-2 expression by the type 1 insulin-like growth factor receptor - the phosphatidylinositol 3-kinase/Akt and Raf/ERK pathways transmit opposing signals. *J Biol Chem* 2004; **279**: 19683–19690.
59 Economou MA, Wu J, Vasilcanu D, Rosengren L, All-Ericsson C, van der Ploeg I *et al.* Inhibition of VEGF secretion and experimental choroidal neovascularization by picropodophyllin (PPP), an inhibitor of the insulin-like growth factor-1 receptor. *Invest Ophthalmol Vis Sci* 2008; **49**: 2620–2626.
60 Wade M, Li YC, Wahl GM. MDM2, MDMX and p53 in oncogenesis and cancer therapy. *Nat Rev Cancer* 2013; **13**: 83–96.
61 Gombos A, Metzger-Filho O, Dal Lago L, Awada-Hussein A. Clinical development of insulin-like growth factor receptor--1 (IGF-1R) inhibitors: at the crossroad? *Invest New Drugs* 2012; **30**: 2433–2442.
62 Salazar-Onfray F, Nakazawa T, Chhajlani V, Petersson M, Karre K, Masucci G *et al.* Synthetic peptides derived from the melanocyte-stimulating hormone receptor MC1R can stimulate HLA-A2-restricted cytotoxic T lymphocytes that recognize naturally processed peptides on human melanoma cells. *Cancer Res* 1997; **57**: 4348–4355.
63 Haapajarvi T, Pitkanen K, Laiho M. Human melanoma cell line UV responses show independency of p53 function. *Cell Growth Differ* 1999; **10**: 163–171.
64 Soussi T. TP53 mutations in human cancer: database reassessment and prospects for the next decade. *Adv Cancer Res* 2011; **110**: 107–139.
65 Houben R, Hesbacher S, Schmid CP, Kauczok CS, Flohr U, Haferkamp S *et al.* High-level expression of wild-type p53 in melanoma cells is frequently associated with inactivity in p53 reporter gene assays. *PLoS One* 2011; **6**: e22096.
66 Dews M, Prisco M, Peruzzi F, Romano G, Morrione A, Baserga R. Domains of the insulin-like growth factor I receptor required for the activation of extracellular signal-regulated kinases. *Endocrinology* 2000; **141**: 1289–1300.
67 Livak KJ, Schmittgen TD. Analysis of relative gene expression data using real-time quantitative PCR and the 2(T)(-Delta Delta C) method. *Methods* 2001; **25**: 402–408.
68 Castro J, Heiden T, Wang N, Tribukait B. Preparation of cell nuclei from fresh tissues for high-quality DNA flow cytometry. *Cytometry* 1993; **14**: 793–804.